Bulk exciton polaritons in GaAs microcavities

Y. Chen
Laboratoire de Microstructures et de Microélectronique, Centre National de la Recherche Scientifique, 196 Avenue Henri Ravera, F-92225 Bagneux, France

A. Tredicucci and F. Bassani
Scuola Normale Superiore, Piazza dei Cavalieri 7, I-56126 Pisa, Italy
(Received 25 January 1995)

The optical properties of excitons in thin layers are significantly different from those in bulk crystals. In particular, we study the case of a bulk material of thickness comparable with the wavelength of the excitonic transition confined on one or on both sides by appropriate Bragg reflectors. If the cavity resonance quasimode is carefully tuned on the excitonic transition, strong exciton-photon coupling takes place and produces a Rabi-like splitting as large as that observed in quantum-well-implanted microcavities and comparable optical absorption. In addition, the polaritonic spatial dispersion and the quantization of the exciton center-of-mass motion introduce remarkable fine structures which are absent in the quantum-well case. We demonstrate the above effects from a spectroscopic analysis of GaAs cavities and compare them with those displayed by quantum-well-implanted microcavities.

I. INTRODUCTION

A growing interest is developing in the optical properties of semiconductor microcavity structures,[1–3] because they can now be produced by advanced crystal-growth technologies such as molecular-beam epitaxy. They allow a control of the photon densities in the optical frequency range similar to that of the more traditional microwave cavities.[4] Particular attention has been focused on the strong coupling between two-dimensional excitons of quantum wells and cavity Fabry-Perot quasimodes.[5–12] A large splitting of mixed exciton-photon modes, namely, the Rabi-like splitting, has been recently observed in quantum-well- (QW-) implanted cavities,[3] showing a great similarity to that due to the atom-field interaction in metallic mirror cavities.[13] Through the design of the QW's and of the dielectric mirrors the exciton transition as well as the Fabry-Perot cavity mode can be tailored to produce enhancement or inhibition of the exciton-photon interaction at the desired frequency. This has stimulated a number of fundamental investigations, and also new application ideas, leading to new types of light-emitting devices, vertical surface emission lasers, bistable optical switching devices, etc.[14]

So far, most of the investigations have been performed on QW implanted planar cavities, where the excitons are sharply localized at the QW location in the growth direction, because they have a larger exciton oscillator strength, and consequently a strong exciton-photon coupling can be obtained. The concept of the interaction between the cavity mode and an electronic excitation mode is, however, a general one and can be extended to other cases different from quantum-well excitons. We have, in fact, proposed a structure in which the cavity mode is resonant with the excitons of the bulk material embedded into the cavity.[15] By carefully tuning the Fabry-Perot quasimode to the bulk exciton transition, an important mode splitting as that observed with QW microcavities can be obtained in spite of the smaller oscillator strength, because of the greater thickness and of the smaller broadening of the 3D excitonic transitions. The cavity structure without QW's is less versatile, because we cannot gauge the transition, but new effects are expected because of the peculiar spatial dispersion of the 3D excitation which produces thin layer polariton interfaces.

The aim of this work is to develop a spectral analysis of GaAs microcavities and to demonstrate the above effects. A close comparison between the GaAs cavity and the QW implanted cavities is presented, and numerical results at normal incidence are derived, to show how to control photon-exciton interactions.

In Sec. II, we present the general theory of linear response of microcavities confined by Bragg mirrors on one or on both sides. In Sec. III, we give numerical results and discussion for the GaAs case. Conclusive remarks are given in Sec. IV.

II. LINEAR OPTICAL RESPONSES OF MICROCAVITY

We consider two types of planar microcavities schematically shown in Fig. 1. The difference between the two are only in their Fabry-Perot construction: (a) is a simple homogeneous layer confined on both sides by distributed Bragg reflectors (DBR's) composed of a sequence of dielectric layers with two different refraction indices; (b) is a similar homogeneous layer confined on one side only. In both cases, the layer thickness is chosen in such a way that the optical-mode frequency is tuned to the bulk exciton resonance (we choose the $n=1$ exciton). We now show how to compute the optical spectra near the resonance frequency for both cases. The procedure is based on enlarged transfer matrices and can be used for

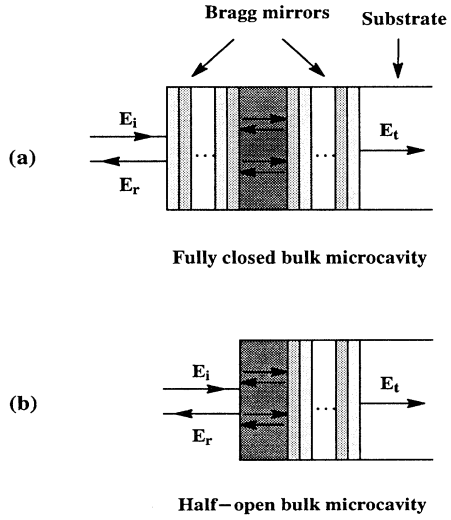

FIG. 1. Schematic representation of two types of planar microcavities: (a) a simple homogeneous layer confined on both sides by Bragg mirrors, composed of a sequence of dielectric layers with two different refraction indices; (b) a similar homogeneous layer, but confined on one side only.

the quantum-well implanted cavities with obvious modifications.[11,16]

First, we consider light propagation in the layer in which the electronic states are off resonance. This is the case of the $\lambda/4$ layers of the Bragg mirrors. The transfer matrix is given for each layer by the expression of classical optics,[17] which, for incidence perpendicular to the layer, is

$$m_j=\begin{bmatrix} \cos\left[\frac{\omega}{c}n_j l_j\right] & -i\frac{1}{n_j}\sin\left[\frac{\omega}{c}n_j l_j\right] \\ -in_j\sin\left[\frac{\omega}{c}n_j l_j\right] & \cos\left[\frac{\omega}{c}n_j l_j\right] \end{bmatrix}, \tag{1}$$

where ω is frequency, c is the speed of light in vacuum, l_j and n_j denote the thickness and refraction index of the jth layer. The material refraction indices can be written as real constant numbers, because we are far from optical resonances.

Second, we consider light propagation in the microcavity when the radiation frequency is close to the exciton resonance ω_0, and include spatial dispersions; the dielectric function is nonlocal in the z direction,[18,19] and we consider its expression in k space, when a one level parabolic exciton band is assumed,

$$\varepsilon(\omega,k)=\varepsilon_\infty+\frac{4\pi\beta\omega_0^2}{\omega_0^2+\hbar k^2/M_{ex}^*-\omega^2-i\Gamma\omega}, \tag{2}$$

where M_{ex}^* is the exciton total effective mass, ω_0 is the zero-momentum exciton energy, $4\pi\beta$ and Γ are the corresponding oscillator strength and transition broadening, respectively. Solving Maxwell's equations with dielectric function (2), we obtain

$$\frac{k^2c^2}{\omega^2}=\varepsilon(\omega,k). \tag{3}$$

This is a standard polariton eigenvalue equation which, because of spatial dispersion, gives rise to two normal modes of propagation, with two different k vectors k_α ($\alpha=1,2$) for each frequency. The electric and magnetic fields of the polariton modes inside the cavity layer can then be expressed as

$$E(z)=\sum_{\alpha=1}^{2}(E_\alpha^+e^{ik_\alpha z}+E_\alpha^-e^{-ik_\alpha z}), \tag{4}$$

$$B(z)=-\sum_{\alpha=1}^{2}\frac{c}{\omega}k_\alpha(E_\alpha^+e^{ik_\alpha z}-E_\alpha^-e^{-ik_\alpha z}), \tag{5}$$

where $E_1^\pm$ and $E_2^\pm$ are four complex field amplitudes, which describe two forward and two backward propagations. Correspondingly, the polarization field can be expressed as

$$P(z)=\sum_{\alpha=1}^{2}\tilde{n}_\alpha^2(E_\alpha^+e^{ik_\alpha z}+E_\alpha^-e^{-ik_\alpha z}), \tag{6}$$

where $\tilde{n}_\alpha^2=c^2k_\alpha^2/\omega^2-\varepsilon_\infty$ corresponds to the exciton contribution to the propagation mode. Assuming zero amplitude of the polarization field at each interface (Pekar's additional boundary condition), i.e., $P=0$, when $z=\pm l_c/2$ (l_c is the cavity thickness), we can set a relation between the four amplitude variables,

$$\begin{bmatrix}E_2^+\\E_2^-\end{bmatrix}=Q_c\begin{bmatrix}E_1^+\\E_1^-\end{bmatrix}, \tag{7}$$

where

$$Q_c=-\frac{\tilde{n}_1^2}{\tilde{n}_2^2}\begin{bmatrix}\lambda_{c2}^* & \lambda_{c2}\\ \lambda_{c2} & \lambda_{c2}^*\end{bmatrix}^{-1}\begin{bmatrix}\lambda_{c1}^* & \lambda_{c1}\\ \lambda_{c1} & \lambda_{c1}^*\end{bmatrix}, \tag{8}$$

and $\lambda_{c\alpha}=\exp(ik_\alpha l_c/2)$, $\lambda_{c\alpha}^*=\exp(-ik_\alpha l_c/2)$. Eliminating the amplitude variables by the values of the electric and magnetic fields at the boundaries, the transfer matrix for the microcavity results in

$$m_c=\left[\begin{bmatrix}\lambda_{c1}^* & \lambda_{c1}\\ \tilde{n}_1\lambda_{c1}^* & -\tilde{n}_1\lambda_{c1}\end{bmatrix}+\begin{bmatrix}\lambda_{c2}^* & \lambda_{c2}\\ \tilde{n}_2\lambda_{c2}^* & -\tilde{n}_2\lambda_{c2}\end{bmatrix}Q_c\right]\times\left[\begin{bmatrix}\lambda_{c1} & \lambda_{c1}^*\\ \tilde{n}_1\lambda_{c1} & -\tilde{n}_1\lambda_{c1}^*\end{bmatrix}+\begin{bmatrix}\lambda_{c2} & \lambda_{c2}^*\\ \tilde{n}_2\lambda_{c2} & -\tilde{n}_2\lambda_{c2}^*\end{bmatrix}Q_c\right]^{-1}. \tag{9}$$

Knowing the transfer matrix of each layer and of the cavity, the total transfer matrix M can be obtained as the product of the individual matrices and reflectance and transmission can be calculated from the expressions

$$r=\frac{M_{21}+n_{sub}M_{22}-M_{11}-n_{sub}M_{12}}{M_{21}+n_{sub}M_{22}+M_{11}+n_{sub}M_{12}}, \tag{10}$$

$$t=\frac{2}{M_{11}+n_{sub}M_{12}+M_{21}+n_{sub}M_{22}}, \tag{11}$$

where n_{sub} is the refraction index of the substrate, which

TABLE I. Parameters used for the numerical calculations of bulk cavity structures.

Exciton energy $\hbar\omega_0$	1515 meV
Exciton broadening parameter Γ	0.1 meV
Exciton effective mass M_{ex}^*	$0.49m_0$
Exciton oscillator strength $4\pi\beta$	1.325×10^{-3}
λ-cavity length l_{GaAs}	232.5 nm
Cavity dielectric constant ε_∞	12.53
AlAs $\lambda/4$ layer thickness l_{AlAs}	65.3 nm
AlAs refraction index n_{AlAs}	$\sqrt{9.8}$
$Al_xGa_{1-x}As$ $\lambda/4$ layer thickness $l_{Al_{0.3}Ga_{0.7}As}$	59.8 nm
$Al_xGa_{1-x}As$ refraction index $n_{Al_{0.3}Ga_{0.7}As}$	$\sqrt{11.7}$

supports our microstructure on one side, and M_{ij} denote matrix elements of M.

III. RESULTS AND DISCUSSION

We calculate linear optical properties of GaAs cavities properly confined on one side or on both sides by Bragg reflectors of the type described in Sec. II. The parameters used for numerical calculations are listed in Table I. For the purpose of comparison, we also compute the linear optical properties of QW implanted microcavities, using the same procedure, but gauging the ω_0 value and taking the limit $M_{ex}^*=\infty$ in the total exciton mass. The parameters chosen for this calculation are reported in Table II. The results of the QW-implanted microcavity agree with those of Andreani *et al.* for the semiclassical case.[11,16]

A. Half-open microcavities

We first examine the phase effect of the Bragg mirror reflection. There are two ways of constructing a dielectric mirror. Let n_1 and n_2 be the refraction indices of the two materials constituent of the Bragg $\lambda/4$ layers. Assuming the growth started with a n_2 layer and ended with a n_1 layer, we have two cases: (i) $n_1>n_2$, (ii) $n_1<n_2$. At the center of the stop band of a Bragg mirror, the reflection coefficient becomes[17]

$$r|_{\omega_0}=\frac{1-n_{sub}(n_1/n_2)^{2N}}{1+n_{sub}(n_1/n_2)^{2N}}, \tag{12}$$

where N is the total number of $\lambda/4$ layers. Clearly, for large N, $r=1$ if $n_1<n_2$ and $r=-1$ if $n_1>n_2$. This means there is a π-phase shift for $n_1>n_2$ reflectors (noted as r^- DBR) and a zero-phase shift for $n_1<n_2$ reflectors (noted as r^+ DBR). Now if a bare cavity layer is grown on one of the two Bragg mirrors, the photon field will be modulated strongly depending on the phase matching with the supporting mirror. This can be used as a way to control the exciton-photon interaction. We show in Fig. 2 the reflectance spectra calculated for a GaAs λ-cavity grown on a Bragg mirror of 20 pairs ($AlAs/Al_{0.3}Ga_{0.7}As$) supported by a thick nonresonant substrate. Both cases of Bragg mirrors, $n_1<n_2$ and $n_1>n_2$ are considered, and resulting spectra are shown to be substantially different. They suggest the following remarks. (i) Since no sharp cavity (photon) mode exist in this case because of the poor reflection at one of the cavity surfaces, no coupled-mode splitting occurs. (ii) The strength of the polariton

TABLE II. Parameters used for the quantum-well implanted cavity structures.[a]

Exciton energy $\hbar\omega_0$	1518 meV
Exciton broadening parameter Γ	0.1 meV
Exciton oscillator strength $4\pi\beta$	3.975×10^{-3}
Quantum-well thickness l_{GaAs}	20.6 nm
λ-cavity length $l_{Al_{0.1}Ga_{0.9}As}$	235.0 nm
Cavity dielectric constant ε_∞	12.1

[a]We use the same parameters of Bragg mirror $\lambda/4$ layers as listed in Table I.

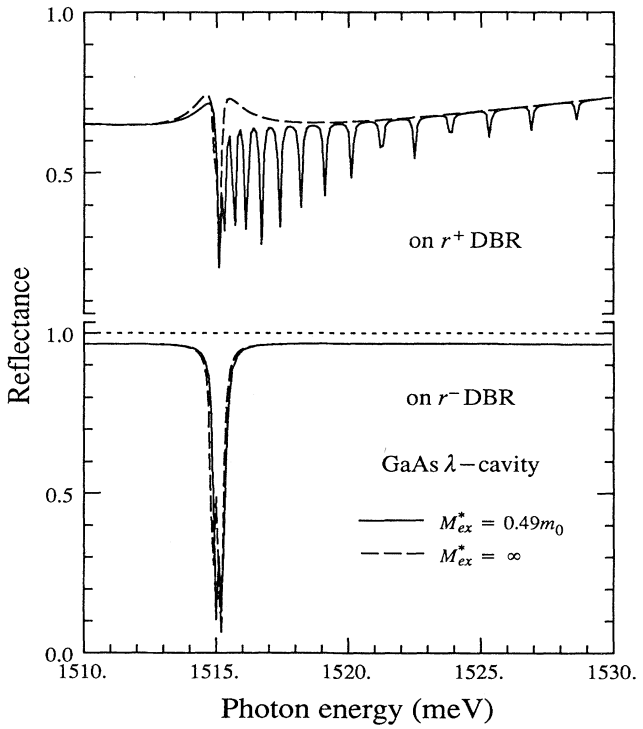

FIG. 2. Reflectance spectra of half-open GaAs λ cavities grown on r^+ (upper curve) and r^- (lower curve) Bragg mirrors.

peaks drastically depends on the sequence of the Bragg pairs: they are enhanced (upper curves) or inhibited (lower curves) only depending on whether the supporting Bragg mirror is r^+ type ($n_1 < n_2$) or r^- type ($n_1 > n_2$). (iii) In the case of polariton enhancement ($n_1 < n_2$), narrow reflection satellite structures appear due to the quantization of the exciton center-of-mass (CM) motion.[18,19] In fact, the cavity polariton reflectance minima are close to the exciton CM quantization energies given by $E_n = \hbar\omega_0 + n^2\hbar^2\pi^2/2M^*_{ex}l_c^2$.

To compare the GaAs-cavity spectra with those of QW ones, we present in Fig. 3 the reflectance spectra calculated using the two above described r^+ and r^- Bragg mirrors and two different quantum-well locations. Comparing the results of Fig. 3 with those of Fig. 2 for the case of GaAs cavity, no exciton CM quantization peaks appear since there is no exciton propagation along the growth direction.

From the above analysis, we observe that the polariton peak amplitudes are not simply related to the exciton oscillator strength. The cavity exciton-photon interaction has to be considered, for instance, using Fermi's golden rule, which takes into account both exciton and photon densities of states. For the GaAs-cavity spectra, for example, we can assume that the exciton function that describes the center-of-mass motion $\psi_{ex}(z)$ and the photon field function $\phi_v(z)$ are slowly varying in comparison with the crystal Bloch functions, so that the atomic scale dipole-field matrix element can be separated and the transition probabilities are proportional to the square of the overlap term,

$$\left| \int \phi_v(z)\psi_{ex}(z)dz \right|^2 . \tag{13}$$

This shows that a selection rule for the cavity polariton originates from the parity of $\phi_v(z)$ and $\psi_{ex}(z)$. Consider for the exciton CM envelope function: $\psi_{ex}(z) = \sqrt{2/l_c}[\cos(n\pi z/l_c), \sin(n\pi z/l_c)], n = [\text{even, odd}]$ integers. Again we have cosine (sine) spatial variation for the optical waves inside the cavity if it is grown on a r^+ (r^-) Bragg reflector. This cavity polariton selection rule explains the structure enhancement or inhibition in the calculated spectra of Fig. 2. Therefore, similarly to the controlled spontaneous emission in microcavity lasers, one can achieve a controlled exciton-photon interaction with the growth of a cavity layer on suitable Bragg reflectors.

B. Fully closed microcavities

We wish now to consider a high-Q-value cavity enclosed by high reflection mirrors on both sides of the Fabry-Perot layer. Due to the cavity *"condensation"* of the optical mode and the resonant tuning to the excitonic transition level, strong coupling between excitons and photons takes place. We present in Fig. 4 the optical spectra near the bulk exciton energy, calculated for a GaAs λ-cavity enclosed by two Bragg mirrors made of 20 pairs (AlAs/$Al_{0.3}Ga_{0.7}As$). We observe the appearance

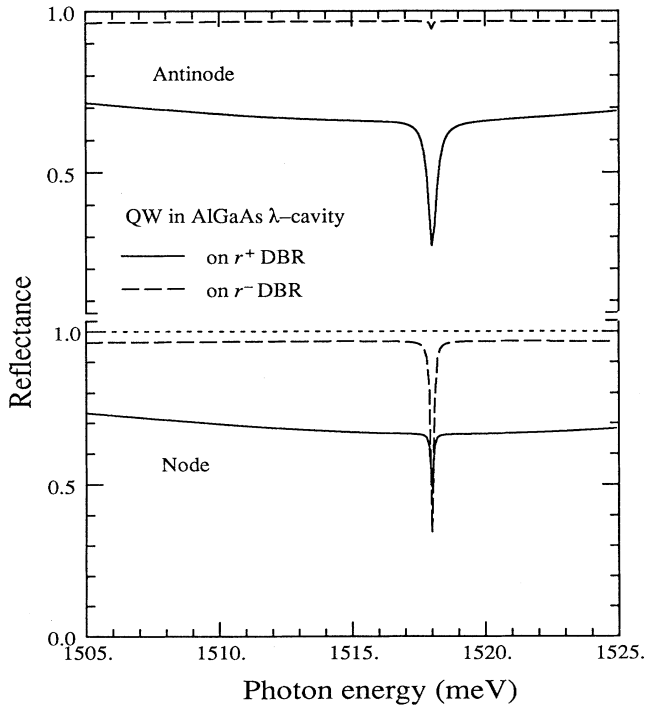

FIG. 3. Reflectance spectra of QW implanted (GaAs/$Al_{0.1}Ga_{0.9}As$) λ cavities grown on r^+ (solid lines) and r^- (dashed lines) Bragg mirrors.

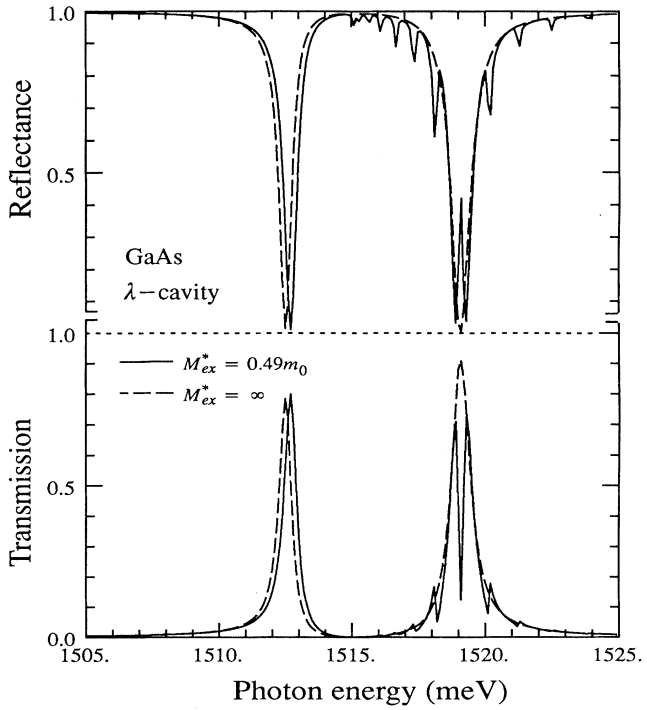

FIG. 4. Reflectance and transmission spectra of a GaAs λ cavity enclosed by two r^+ Bragg mirrors. Solid and dashed curves show, respectively, the results of using finite and infinite mass excitons.

of two dominant transition peaks with a satellite structure above the bulk exciton energy. We attribute these two main peaks to the cavity mode and $n=1$ exciton mode so strongly coupled to become the two new mixed normal modes. The normal-mode splitting, ΔE_{Rabi}, is typically Rabi-like, and, in the limit of totally reflecting and not distributed mirrors, can be considered as the bulk polariton mode splitting at the exciton-photon dispersion cross point. We note that the polariton splitting at the cross point, $2\omega_c=\sqrt{4\pi\beta/\varepsilon_\infty}\omega_0$, is at least 100 times larger than the so-called longitudinal-transverse splitting, ΔE_{LT}. The polariton splitting at the exciton-photon cross point cannot be detected in the bulk because of the very small and unstructured density of states. Since polaritons in bulk crystal are stationary states, each polariton propagates independently with well-defined energy and wave vector, because of the conservation of the crystal momentum. In a thin layer, the crystal translational invariance breaks down and polariton interference occurs, which leads to *coupled mode* standing waves or quantized polariton states.[18,19] Therefore, the cavity polariton mode splitting is experimentally observable. So far, only in a QW implanted cavity the Rabi-like splitting has been measured.[3] Theoretical investigations have shown that the Rabi splitting in QW cavities can be analyzed using a semiclassical linear dispersion theory or the full quantum theory.[11] They are both equivalent to our transfer-matrix formalism adapted to a QW cavity. We have calculated the Rabi splitting as a function of exciton oscillator strength in both cases of a bulk cavity and of a QW implanted cavity. Figure 5 shows both results, where for the comparison we have only considered the exciton main peak. It can be noticed that the mode splitting in a bulk GaAs cavity is much more dependent on the exciton oscillator strength than in the QW cavity. This can be traced to the difference in the excitonic active layer thicknesses appearing in the transfer-matrix expressions (8) and (9). While the difference in oscillator strength dependence is only quantitative, new features also appear in the bulk cavities; most of all fine structures

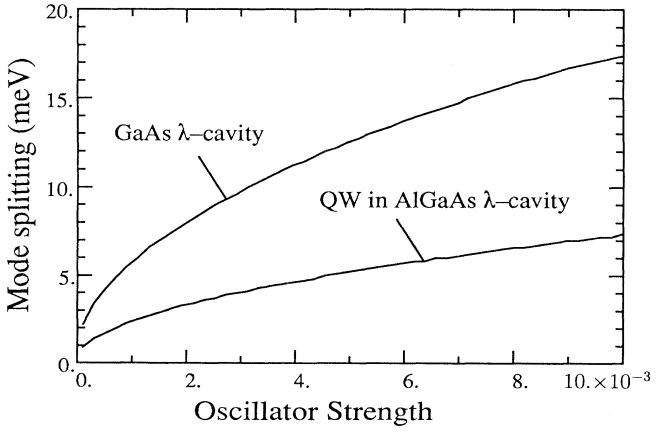

FIG. 5. Normal mode splitting as a function of exciton oscillator strength for a GaAs λ cavity and a QW implanted ($GaAs/Al_{0.1}Ga_{0.9}As$) λ cavity.

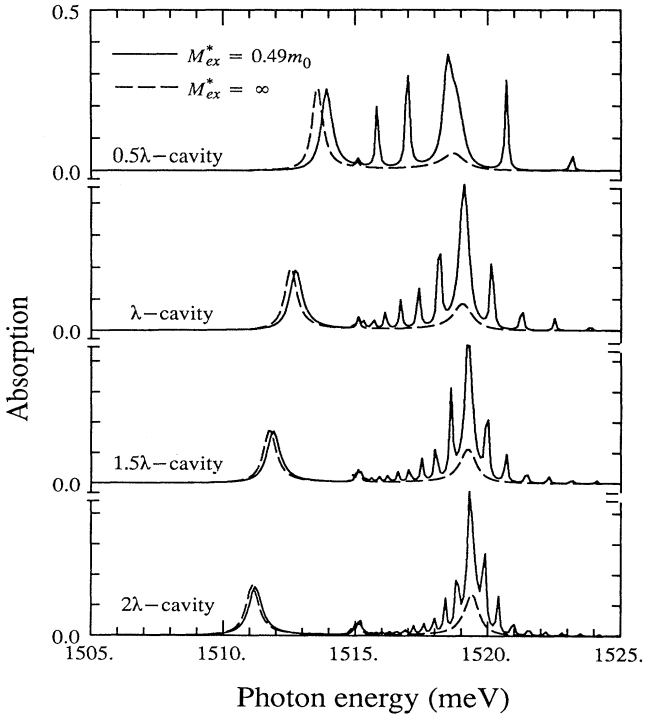

FIG. 6. Absorption spectra of GaAs λ/2, λ, 3λ/2, and 2λ cavities. Solid and dashed lines show, respectively, the results of using finite and infinite mass excitons.

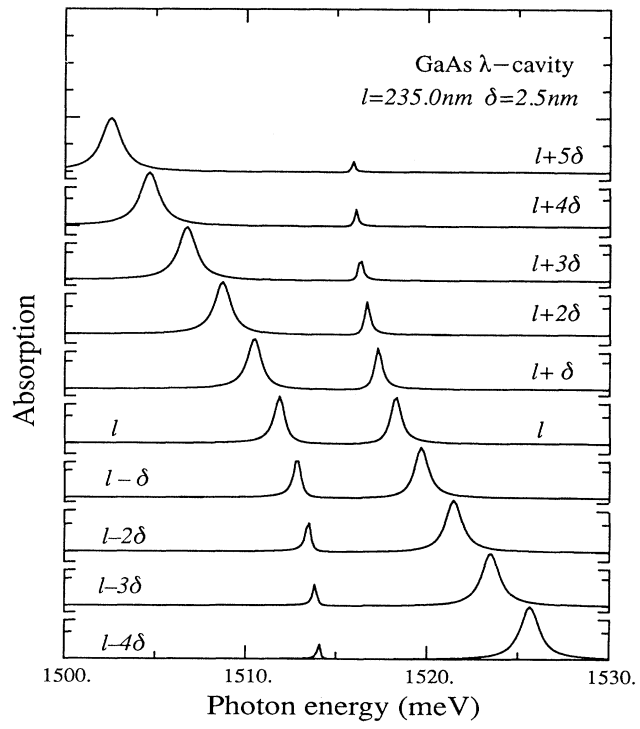

FIG. 7. Absorption spectra of GaAs λ cavities under different resonance conditions, obtained with infinite mass excitons.

above the bulk exciton energy, which have the same origin as those of the half-open cavities. They appear more clearly in this case, as can be seen in the absorption spectra reported in Fig. 6 for the cases of $\lambda/2$, λ, $3\lambda/2$, and 2λ thick GaAs cavities. It shows that the exciton fine structure varies progressively, following the law of the exciton CM quantization as a function of layer thicknesses. A further qualitative difference is the increase of the mode splitting as the cavity length increases, opposite to the case of QW implanted cavities. This is because in the case of QW implanted cavities, increasing the cavity length does not affect the oscillator strength per unit area so that the normal-mode splitting does not increase (in fact, a slight decrease can be expected because of the decrease of the optical-mode density). In contrast, in the case of bulk GaAs cavities, the whole body of the cavity is affected and increasing the cavity length leads to an increase of the exciton oscillator strength per area, giving rise to an increased normal-mode splitting.

Similar to the detuning behavior in QW implanted cavities, the GaAs cavity mode interaction critically depends on the resonant condition, i.e., the level matching between the exciton transition energy and the photonic quasimode. To illustrate this effect, we show in Fig. 7 the absorption spectra of a GaAs λ cavity under different resonance conditions, corresponding to different detuning.

Finally, we would like to mention that the calculation presented in this work is a simple version, which can be improved by including more material and refining the physical model of the exciton polariton. To compare the calculated quantized energy levels with experimental data, for instance, the effective exciton confinement thickness must be smaller than the cavity length, because of the exciton dead layers near the cavity surfaces, typically of the order of the exciton Bohr radius.[19–21]

IV. CONCLUSIONS

The main result of this work is to suggest a type of active microcavity tuned to the main bulk exciton resonance. The case of GaAs is considered including spatial dispersion, and the results are compared with those of QW implanted microcavities. It is shown that the exciton-photon interaction can be substantially modulated even in the case of half-open cavities (bad Q-value cavities). Enhanced or inhibited exciton-photon coupling can be obtained by appropriate conditions on the Bragg mirrors. In the case of fully enclosed microcavities, a Rabi-like splitting appears, which increases as the oscillator strength and the cavity length increase. In addition to the Rabi-splitted normal modes, satellite structures appear in the optical spectra, due to the quantization of the exciton center-of-mass motion. These properties make the above proposed type of cavity systems of potential interest for studying the phenomena and for possible applications, particularly in nonlinear optics.

ACKNOWLEDGMENTS

This work is partially supported by the French and Italian Ministries of Foreign Affairs through the Galileo program.

[1]H. Yokoyama, Science **256**, 66 (1992), and references therein.
[2]Y. Yamamoto and R. E. Slucher, Phys. Today **46** (6), 66 (1993).
[3]C. Weisbuch, M. Nishioka, A. Ishikawa, and Y. Arakawa, Phys. Rev. Lett. **69**, 3314 (1992).
[4]S. Haroche and D. Kelppner, Phys. Today **42** (1), 24 (1989).
[5]Y. Yamamoto, F. Matinaga, S. Machida, A. Karlsson, J. Jacobson, G. Björk, and T. Mukai, J. Phys. (France) IV **5**, C39 (1993).
[6]R. Houdré, R. P. Stanley, U. Oesterle, and M. Ilegems, and C. Weisbuch, J. Phys. (France) IV **5**, C51 (1993).
[7]V. Savona, Z. Hradil, A. Quattropani, and P. Schwendimann, Phys. Rev. B **49**, 8774 (1994).
[8]R. Houdré, C. Weisbuch, R. P. Stanley, U. Oesterle, P. Pellandini, and M. Ilegems, Phys. Rev. Lett. **73**, 2043 (1994).
[9]S. Pau, G. Björk, J. Jacobson, H. Cao, and Y. Yamamoto, Phys. Rev. B **51**, 7090 (1995).
[10]I. Abram, S. Iung, R. Kuzelewicz, G. Le Roux, C. Licoppe, L. J. Oudar, E. V. K. Rao, J. Bloch, R. Planel, and V. Thierry-Mieg, Appl. Phys. Lett. **65**, 2516 (1994).
[11]L. C. Andreani, V. Savona, P. Schwendimann, and A. Quattropani, Superlatt. Microstruct. **15**, 453 (1994).
[12]V. Savona, L. C. Andreani, P. Schwendimann, and A. Quattropani, Solid State Commun. **93**, 733 (1995).
[13]Yifu Zhu, D. J. Gauthier, S. E. Morin, Quilin Wu, H. J. Carmichael, and T. W. Mossberg, Phys. Rev. Lett. **64**, 2499 (1990).
[14]Opt. Quantum Electron. **24** (1992), special issue on microresonator devices, edited by J. Jewell.
[15]Y. Chen, A. Tredicucci, and F. Bassani, J. Phys. (France) IV **5**, C453 (1993).
[16]L. C. Andreani, Phys. Lett. A **192**, 99 (1994).
[17]M. Born and F. Wolf, *Principles of Optics* (Pergamon, New York, 1980).
[18]Y. Chen, F. Bassani, J. Massies, C. Deparis, and G. Neu, Europhys. Lett. **14**, 483 (1991).
[19]A. Tredicucci, Y. Chen, F. Bassani, J. Masseis, G. Neu, and C. Deparis, Phys. Rev. B **47**, 10438 (1993).
[20]J. J. Hopfield and D. G. Thomas, Phys. Rev. **132**, 563 (1963).
[21]F. Bassani, Y. Chen, G. Czajkowski, and A. Tredicucci, Phys. Status Solidi B **180**, 115 (1993).

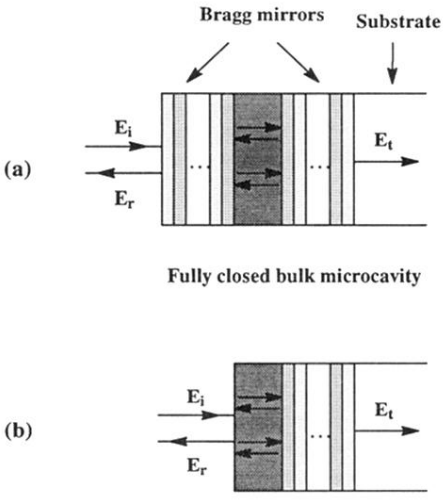

FIG. 1. Schematic representation of two types of planar microcavities: (a) a simple homogeneous layer confined on both sides by Bragg mirrors, composed of a sequence of dielectric layers with two different refraction indices; (b) a similar homogeneous layer, but confined on one side only.